Extension of NVNA Baseband Measurement for Power Amplifier and Mixer Characterization under Complex Modulation

Yichi ZHANG, Xiaotao GUO, Zhao HE, Lifeng WANG, Wei ZHAO, Zilong ZHANG

***Abstract* — ~~This paper~~We have investigated~~s~~ the baseband measurement techniques of the nonlinear vector network analyzer (NVNA) test bench, aiming to fully characterize the behaviors of RF power amplifiers and mixers under complex modulation. In order to involve the baseband measurement, two kinds of NVNA phase reference approaches are developed as alternative solutions, so that the baseband phase measurements can be synchronized with those of modulated components at fundamental and harmonic bands. In the first case, a modulated baseband signal is combined with another modulated multi-harmonic one to become the desired NVNA phase reference. While in the other case, a sweeping multisine is used as the primary phase reference, and assisted by an auxiliary one to obtain equivalently static NVNA phase measurements. To validate the proposed NVNA test bench, an RF power amplifier is tested by applying a large-signal LTE-like multisine drive, whose multi-band output measurements are compared with that using an oscilloscope. Moreover, an RF mixer is used as a second type of device under test to explore the application of this work.**

***Index Terms* — nonlinear vector network analyzer (NVNA), phase reference, baseband measurement, power amplifier, mixer**

I. Introduction

ALONG with the rapid development of high-speed wireless communication, there has been a driving force in advancing various radio frequency (RF) and microwave measurement techniques. Accurate characterization of RF devices, such as power amplifiers (PA) and mixers, are the keys for linear and nonlinear measurement-based modeling, and have enabled high-efficiency design and optimization in practice for engineers. To address the need of future communication systems, whose devices will work under broadband complex modulations, novel measurement techniques and test benches are expected for and to assist with the large-signal nonlinear behavior characterization.

During the past decade, the mixer-based nonlinear vector network analyzer (NVNA) is proposed and used for characterizing wideband signals and nonlinear devices [1]. With the use of a phase reference, which is generally applied by an accessory comb/impulse generator, the NVNA architecture is empowered for measuring both magnitude and phase spectra of a complex RF signal. In practice, commercial NVNAs of this kind have been widely used for X-parameter modeling and associated applications, which are mainly based on harmonic nonlinearity characterization [2]-[4].

Recently, different ideas have been proposed to further develop NVNA test benches for dense-spectral-grid modulated measurements [5]-[17]. On one hand, novel types of phase reference signals are put forward to break through the spectral grid limitation [6]-[13] [15]-[17]. On the other hand, novel calibration methods and standards are presented [5] [6] [8] [10]-[17]. To date, the NVNA test benches have been empowered for characterizing the complex multi-harmonic inter-modulation behavior of an RF PA on dense spectral grids [16] [17].

To the best of our knowledge, however, the baseband measurement of NVNA test benches has not been given adequate attention to or fully utilized until now. As a result the baseband behavior, which is of great significance to the temporal current and voltage (*I*-*V*) waveform analysis, of a device under test (DUT) is always neglected when characterizing its nonlinear distortion under large-signal modulated conditions [15]-[17]. Compared with the full-band time-domain characterization using oscilloscopes, the last missing piece to complete NVNA techniques is the extension of baseband measurement upon the basis of existing work from our point of view.

This paper mainly investigates the baseband measurement techniques of the NVNA test bench, aiming to fully characterize the behaviors of RF power amplifiers and mixers under complex modulation. To involve the desired baseband measurement, two kinds of NVNA phase reference approaches are developed as alternative solutions. In the first case, a modulated baseband signal is combined with another modulated multi-harmonic one to become the desired phase reference. While, in the second case, a sweeping multisine is elaborately controlled, and serves as an equivalently static NVNA phase reference desired. Besides the popular PA characterization for most NVNA test benches [1]-[4] [6] [7] [16] [17], an RF mixer is tested as a second type of DUT to explore the application of this work

In the following sections, the measurement principle and calibration techniques of NVNA test benches are briefly reviewed in Section II. As the main novelty and contribution of this work, the development of NVNA baseband measurement is introduced in depth in Section III. The validation and application of proposed methods is given in Sections IV and V. Discussions are presented in Sections VI.

Project funded by China Postdoctoral Science Foundation (2014M560106 & 2015T80118) and National Key Technologies R&D Program of China (2014BAK02B04)

Yichi ZHANG, Xiaotao GUO, Zhao HE, Lifeng WANG, Wei ZHAO, and Zilong ZHANG are with the National Institute of Metrology (NIM), Beijing, China (e-mail: zhangyichi@nim.ac.cn).

II. NVNA Measurement and Calibration

A. Test Bench and Measurement Principle

The block diagram and signal flow of an NVNA test bench are shown in Fig. 1. The four-port vector network analyzer (VNA) operates in the receiver mode, and offers five (or more) synchronous receiver channels for signal measurement. Among these receivers, those of Port 1 and Port 2 are used for incident and scattered wave measurement of the DUT, while that of Port 3 is used for the phase reference. In order to achieve modulated DUT characterization, an external vector signal generator (VSG) has to be used for applying the desired periodical stimulus. Moreover, a proper phase reference signal is needed, which is required to offer stable spectral components at all frequency points under test.

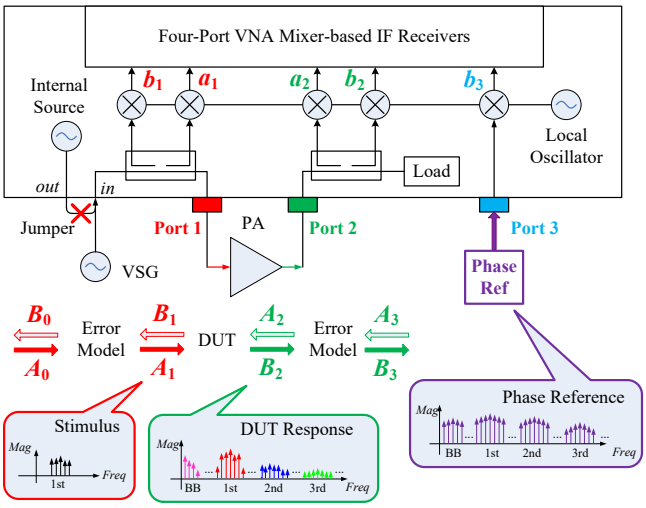

Fig. 1. Block diagram and signal flow of an NVNA test bench. The internal sources of VNA are all powered off. The modulated stimulus is applied through the "Source In" connector of front-panel jumper. Note that Port 1, Port 2 and Port 3 are, respectively, chosen for DUT input/output and phase reference measurements in this paper, where a_1, b_1, a_2, b_2, and b_3 denote corresponding receiver channels of VNA.

According to (1), the phase reference signal (denoted by R) plays a very significant role during NVNA measurement, by offering a static phase measurement at each frequency point. Hence both the random contribution φ_{lo} arising from local oscillator and the time-variant term $2\pi ft$ can be removed from a single-receiver measurement based on down-conversion [18]. In this way, all the spectral components of a signal under test can be sweepingly measured one after another.

$$\begin{aligned} \angle a_1 &= \angle A_1 - \varphi_{lo} - 2\pi ft = \text{Random} \quad , \\ \angle b_3 &= \angle R - \varphi_{lo} - 2\pi ft = \text{Random} \quad , \\ \angle A_0 &= \angle a_1 - \angle b_3 = \angle A_1 - \angle R = \text{Constant} \quad . \end{aligned} \tag{1}$$

As a consequence, the raw NVNA measurements (A_0, B_0, A_3, B_3) of a two-port DUT, e.g. an RF PA, can be obtained based on the complex-valued raw measurements of five receivers (a_1, b_1, a_2, b_2 and b_3) as shown in (2).

$$\begin{aligned} A_0 &= a_1 \cdot \frac{|b_3|}{b_3} = |a_1| \angle (a_1 / b_3), \\ B_0 &= b_1 \cdot \frac{|b_3|}{b_3} = |b_1| \angle (b_1 / b_3), \\ A_3 &= a_2 \cdot \frac{|b_3|}{b_3} = |a_2| \angle (a_2 / b_3), \\ B_3 &= b_2 \cdot \frac{|b_3|}{b_3} = |b_2| \angle (b_2 / b_3), \end{aligned} \tag{2}$$

B. NVNA Calibration

Based on an eight-term error model (as shown in Fig. 2) and corresponding calibration techniques, the effective NVNA measurements (A_1, B_1, A_2, B_2) can be derived upon raw measurements (A_0, B_0, A_3, B_3). As shown in (3) and (4), e_{00}, e_{11}, e_{01}, e_{10}, e_{33}, e_{22}, e_{32}, and e_{23} denote the complex-valued original coefficients of eight-term error model, and establish the vector correction relationship between NVNA raw and effective measurements, while Δx, Δy and k are derived quantities for simplified expression [1].

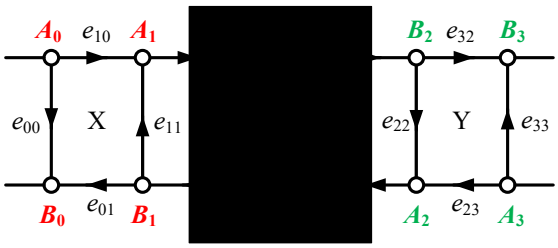

Fig. 2. Illustration of eight-term error model.

$$\begin{bmatrix} A_1 \\ B_1 \\ A_2 \\ B_2 \end{bmatrix} = \frac{1}{e_{01}} \begin{bmatrix} -\Delta x & e_{11} & 0 & 0 \\ -e_{00} & 1 & 0 & 0 \\ 0 & 0 & -k\Delta y & ke_{22} \\ 0 & 0 & -ke_{33} & k \end{bmatrix} \begin{bmatrix} A_0 \\ B_0 \\ A_3 \\ B_3 \end{bmatrix} , \tag{3}$$

$$\begin{aligned} \Delta x &= e_{00}e_{11} - e_{01}e_{10} \\ \Delta y &= e_{33}e_{22} - e_{32}e_{23} \quad . \\ k &= e_{01}/e_{32} \end{aligned} \tag{4}$$

NVNA test benches require thorough (short, open, load, thru, power and phase) calibrations to find all the eight error model coefficients, rather than incomplete ones as VNA demands [1]. After classic two-port relative short-open-load-thru (SOLT) calibration, the complex-valued e_{01} is left unknown for further determination. Then power and phase calibrations are needed to determine the modulus and angle, respectively, of e_{01} at each frequency point. Detailed introduction and discussion of classic

NVNA calibration can be found in [1] [19] [20].

To achieve multi-band NVNA phase calibration on dense spectral grids, an alignment-based multi-step phase calibration method is proposed in [17], so that the limitation of a single phase standard can be overcome. Using a group of dual-band signals as phase standards, this method calibrates two test (sub-) bands at once, and stitches the calibration results together after proper phase alignments to become a complete one. In this paper, the same phase calibration method is applied to our NVNA test bench.

III. Extension of NVNA Baseband Measurement

As mentioned in Section II (A), the NVNA phase reference signal is required to offer stable spectral components at all frequency points under test. To deal with the extension of baseband measurement, the design and realization of desired phase reference in this paper needs to meet the following requirements:

(i) involvement of both baseband and multi-harmonic components, so that the full spectral behavior of a nonlinear DUT can be inspected;

(ii) wide test bands on dense spectral grids, so that more than tens of spectral components are measurable for nonlinear DUT characterization under complex modulation.

As alternative solutions of above challenges, two kinds of approaches are proposed next.

A. Solution One

As shown in Fig. 3, the first approach of obtaining desired NVNA phase reference is by combining two modulated signals together. One signal deals with the baseband components of interest, which can be generated as a user-defined pulsed-RF or multisine with a low-frequency carrier. While the other one deals with multi-harmonic modulated components. According to the previous work in [5], [10], [11], [14], [16], and [17], potential solutions of the second signal can be chosen from using (i) pseudo-random binary sequence or chirp "triggered" comb generator and (ii) pulsed-RF or multisine driven step recovery diode (SRD) comb generator. Despite the detailed difference in impulse generation, the basic principle of all above solutions is to disturb the impulse train into a non-equally spaced one, so that modulated components at each harmonic band can be obtained.

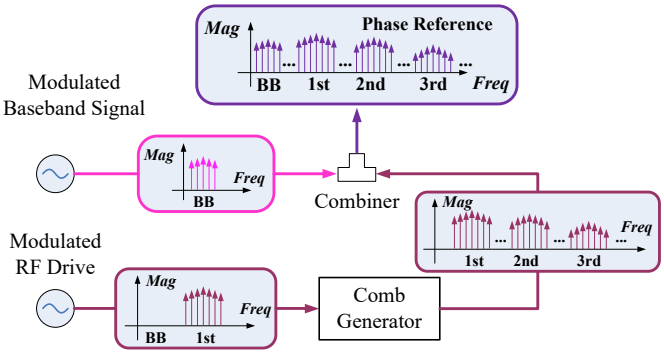

Fig. 3. Illustration of phase reference generation

Without loss of generality, pulsed-RF signals are used in this section to generate the desired NVNA phase reference, so that one can clearly distinguish the baseband and multi-harmonic contributions in the time-domain waveform. As shown in Fig. 4, the temporal waveform of derived phase reference contains two segments apart with the same duty cycle of 1% (25 ns in duration). The smaller-signal segment is the contribution of baseband components, where a carrier frequency of 20 MHz is used. As a result, only a half period of the carrier can be generated within the pulse duration. The larger-signal segment is the contribution of harmonic components, where a carrier frequency of 1 GHz is used to drive the SRD comb generator. Hence a short impulse train is derived.

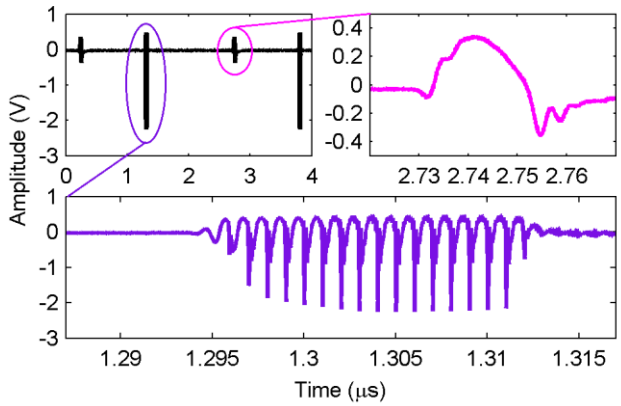

Fig. 4. Temporal waveform of derived phase reference signal based on pulsed-RF signals. The upper left shows the entire period (2.5 μs) of phase reference. The upper right shows the contribution of baseband components, while the lower shows that of harmonic ones.

In Fig. 5, the spectral components of above phase reference are shown at the baseband and harmonic bands. Due to the pulsed modulation, the bandwidth of main-lobe baseband components is more than 40 MHz, where a power level over -80 dBm is available on a spectral grid of 400 kHz. Within the fundamental and harmonic bands, the bandwidths are more than 60 MHz, and the available power level is above -70 dBm. In this way, the desired NVNA phase reference signal is obtained.

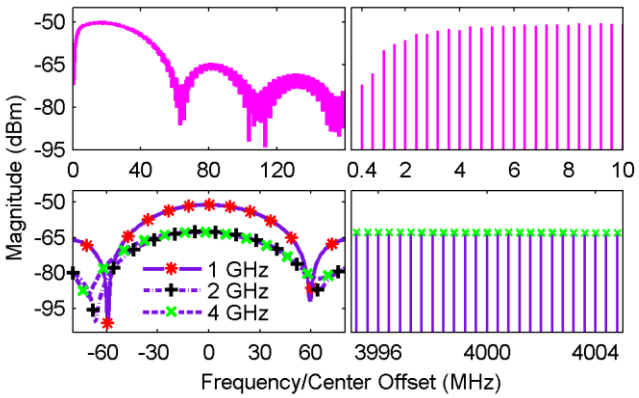

Fig. 5. Spectral magnitude of the phase reference. The upper ones show the overall (left) and zoomed-in (right) baseband spectra, while the lower ones show the overall (left) and zoomed-in (right) harmonic spectra.

It is worth mentioning that the performance (e.g., the bandwidth, spectral grid, and power level) of this phase reference approach can be largely enhanced by using other types of modulated signals. In [16], a modulation bandwidth of 160 MHz, which can be further multiplied at harmonic bands, has been experimentally confirmed on a dense spectral grid down to a few kHz, along with the power level up to -50 dBm. According to the actual experimental conditions, one can freely chose the satisfactory modulated signals to achieve the desired NVNA phase reference in fact.

B. Solution Two

As shown in Fig. 6, the second approach of achieving desired NVNA measurement is by using a sweeping multisine on dense spectral grids as the primary phase reference, and adding an extra reference signal on coarse grids as the auxiliary one. When using a commercial VSG to generate the sweeping multisine, the carrier phase is randomly assigned, just like that of the VNA local oscillator. As a result, the sweeping multisine cannot serve as a static phase reference on its own. However, the random phase offset of carrier identically change the phase of each tone, due to the principle of I/Q modulation. For example, when the baseband multisine sweeps back from harmonics to the very baseband, the phases of all components are changed with the same unknown offset. Taking full advantage of this feature, an auxiliary phase reference on coarse spectral grids is added to the test bench in this paper, so that the random phase offset of "sweeping" carrier can be measured and compensated, obtaining an equivalently static NVNA phase reference desired. With loss of generality, the auxiliary signal can be derived using the commercial NVNA comb generator on 10-MHz spectral grid directly, or by combining a continuous wave (CW) driven SRD comb generator and the 10-MHz reference of test bench.

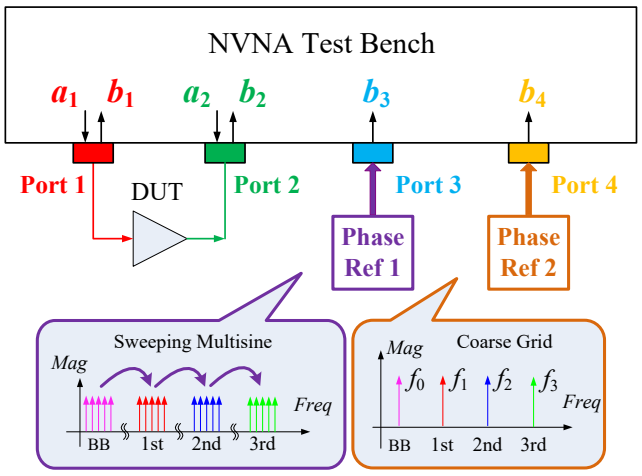

Fig. 6. Illustration of NVNA test bench based on sweeping multisine phase reference.

As a matter of fact, several processing methods, which are almost equivalent but slightly different in details, are optional for the proposed test bench. From our perspectives, the most convenient one can be introduced step by step as follows. To simplify the discussion, here we assume that the bandwidth of a single multisine reference is sufficient for each test band at baseband and harmonics.

- Firstly, the multisine phase reference starts from baseband, and keeps static when the NVNA test bench sweepingly measures a_1, b_1, a_2, b_2, b_3 and b_4 at each tone of interest inside the baseband. At the baseband frequency of auxiliary reference, e.g., f_0=10 MHz, the phase offset $\Delta\varphi_0$ of baseband measurements can be determined as

$$\Delta\varphi_0 = \angle\left[b_3(f_0)/b_4(f_0)\right] \quad . \tag{5}$$

In this way, the raw NVNA phase measurements at each tone inside the baseband can be corrected from (2) to

$$\begin{aligned} \angle A_0 &= \angle(a_1/b_3) + \Delta\varphi_0, \\ \angle B_0 &= \angle(b_1/b_3) + \Delta\varphi_0, \\ \angle A_3 &= \angle(a_2/b_3) + \Delta\varphi_0, \\ \angle B_3 &= \angle(b_2/b_3) + \Delta\varphi_0 . \end{aligned} \tag{6}$$

- Right after the last-tone measurement of baseband is finished, the multisine phase reference sweeps from baseband to the fundamental test band by switching the carrier frequency but without changing the I/Q signals. As a matter of fact, the very I/Q signals should be continuously played during the entire experiment (including the calibration procedure), and be disturbed at no time. Afterwards, the multisine reference keeps static again when the NVNA test bench sweepingly measures a_1, b_1, a_2, b_2, b_3 and b_4 at each tone of interest inside the

fundamental band. At the fundamental frequency of auxiliary reference, e.g., f_1=1 GHz, the phase offset $\Delta\varphi_1$ of fundamental measurements can be determined by using (5) as well and changing the subscript from 0 to 1. Similarly, the raw phase measurements can be corrected referring to (6).

- In the same way, higher harmonic bands can be measured one after another, under the elaborate control of VNA and multisine reference "sweep." After the highest test band is finished, the multisine phase reference sweeps back to the baseband, and repeats the same procedure over and over again. Following the corrections shown in (5) and (6), an equivalently static NVNA phase reference desired can be obtained, as long as the auxiliary phase reference and multisine I/Q signals keep static.

To validate above method, the phase stability of our NVNA test bench measurements is experimentally inspected, and compared with that of alternative solution discussed in Section III (A). As shown in Fig. 7, the random errors of both solutions are generally less than ±0.4 deg.. Hence the validity of both approaches can be confirmed.

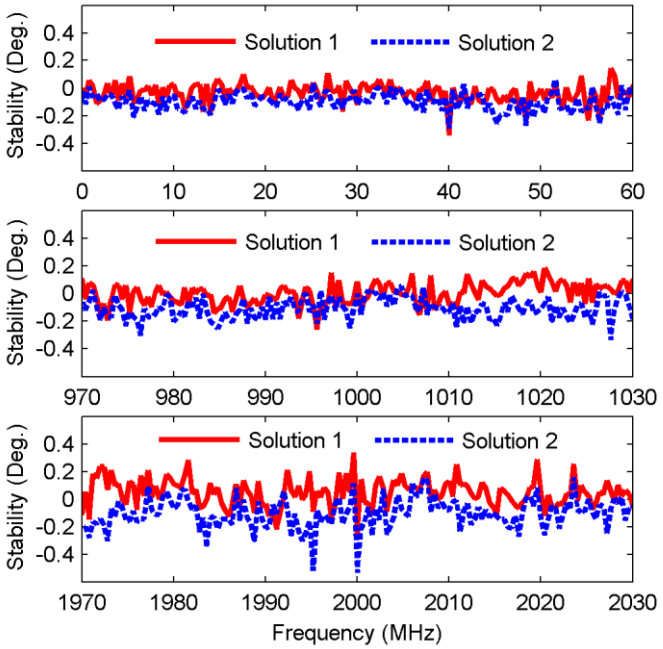

Fig. 7. Stability of test bench phase measurements at the baseband (upper), fundamental (middle), and second harmonic (lower) test bands. Note that this result reflects the deviation between sequential phase measurements, which contains the contributions arising from both phase reference and DUT.

IV. PA Characterization

A. Experimental Condition

In this section, an RF PA under large-signal modulated stimulus is measured using our NVNA test bench, so that the validity of proposed methods can be further verified, and the significance of baseband measurement can be inspected. To achieve the test bench as shown in Fig. 1, a four-port Rohde & Schwarz ZVA8 VNA is used in this paper. Due to its minimum frequency limit and for the purpose of convenient processing, a spectral grid of 400 kHz is chosen for the experiments. As a result, the desired period of modulated test stimulus is determined as 2.5 μs. According to the DUT (Mini-Circuit ZFL-11AD+) specifications, a center frequency of 1 GHz is used for modulated stimulus generation.

In order to obtain a long term evolution (LTE-) like stimulus, a real LTE signal with 20 MHz bandwidth is generated using a VSG in this paper, and measured by an oscilloscope in advance. Based on the fast Fourier transformation (FFT) of truncated measurements, whose time span is 2.5 μs as mentioned above, the phase and magnitude spectra of desired periodical stimulus can be derived. Then an LTE-like multisine stimulus can be generated with the VSG under user-defined I/Q modulation. In Fig. 8, the waveforms of original LTE signal and derived LTE-like multisine, along with the phase and magnitude spectra based on truncated measurements, are shown to illustrate the procedure.

In the following sub-section, the frequency- and time-domain NVNA measurements of the DUT output are given, and compared with those using an oscilloscope.

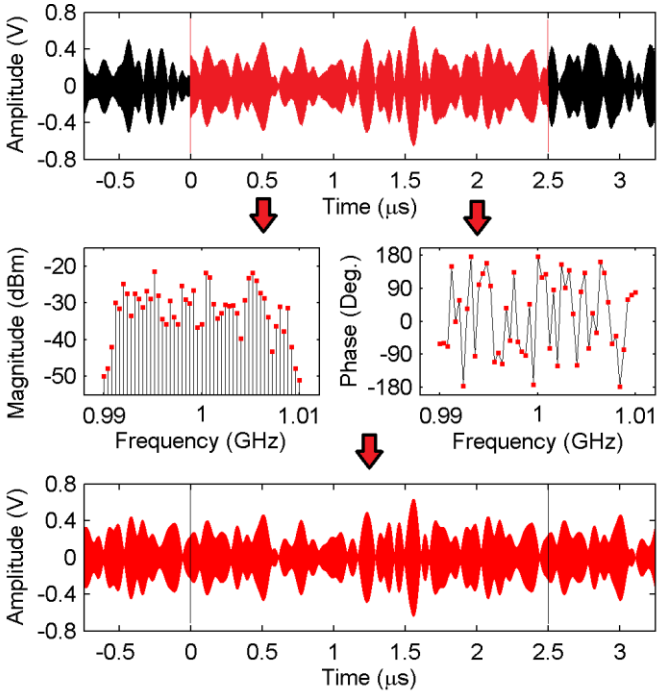

Fig. 8. Waveforms (upper and lower ones) and spectra (middle ones) of the original LTE signal (upper) and LTE-like multisine stimulus (lower).

B. Frequency-domain Measurement

As shown in Fig. 9, the DUT shows obvious baseband, multi-harmonic, and inter-modulation nonlinearities under the experimental condition in this paper. In the baseband, the bandwidth of dominant components is up to 15 MHz, with a power level range from -50 dBm to -20 dBm approximately. In the fundamental band, the maximum power level increases to about -10 dBm inside the 20-MHz stimulus band, and the adjacent channel power ratio (ACPR) degrades from more than

50 dB to only 20 dB. Moreover, the power levels of second harmonic components increase from −90 dBm to −30 dBm. As a result, a desired experimental circumstance is obtained for validating our NVNA test bench and the proposed phase reference approach.

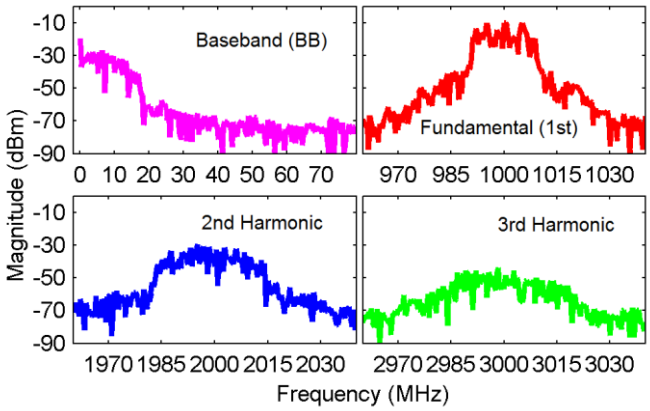

Fig. 9. Magnitude measurements of PA output (B_2) using NVNA test bench.

According to the experimental results given in Fig. 10, where the NVNA measurements are compared with those of an oscilloscope, the magnitude deviation is less than ±0.2 dB in both the baseband and fundamental bands, and less than ±0.5 dB in second harmonic band. For phase measurements on the other band, the deviation is generally less than ±2 deg. in both the baseband and fundamental bands, and less than ±4 deg. in second harmonic band, as shown in Fig. 11. As a result, the validity and accuracy of our NVNA test bench are confirmed.

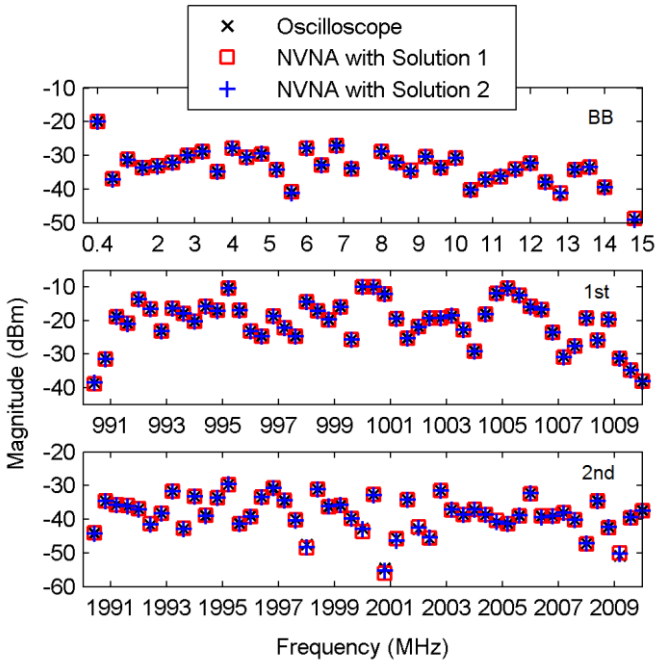

Fig. 10. Comparison between magnitude measurements of PA output (B_2) using oscilloscope and NVNA test bench.

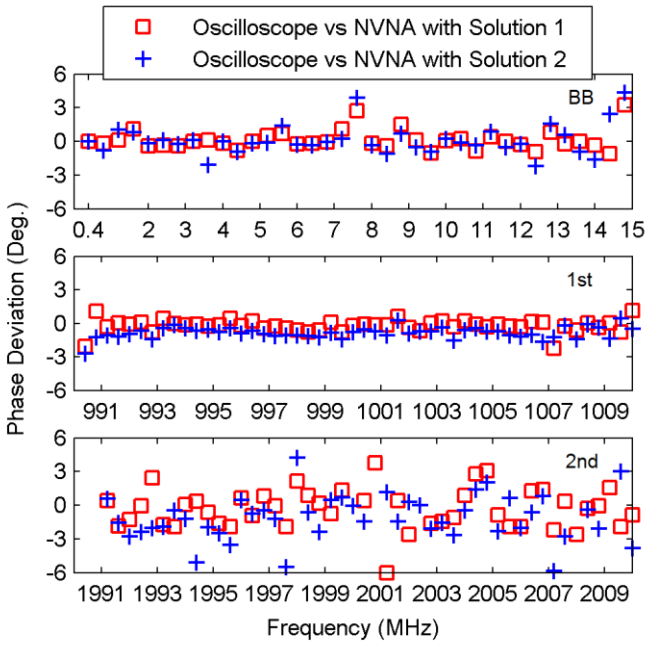

Fig. 11. Comparison between phase measurements of PA output (B_2) using oscilloscope and NVNA test bench.

To better reveal the phase measurement accuracy, Fig. 12 shows the relationship between the phase deviation in Fig. 11 and the power level under test in Fig. 10. One can clearly see that, the phase measurement error increases roughly when the power level drops. From our point of view, this phenomenon is the total contribution of DUT instability, calibration errors, dynamic ranges, and random effects. Despite all this, a good phase accuracy of ±2 deg. can be guaranteed for the dominant components (-35 dBm or above) of DUT output.

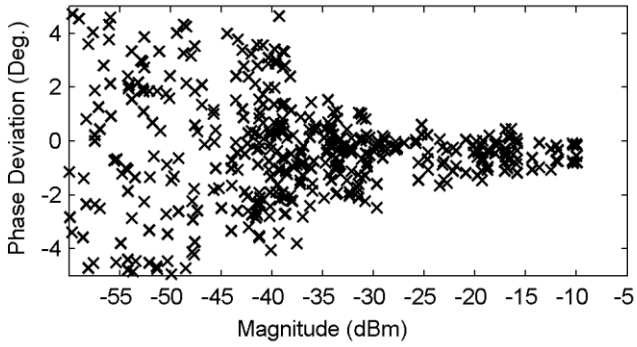

Fig. 12. Deviation of phase measurements versus the magnitude under test

C. Time-domain Comparison

In the time domain, the reconstructed DUT output wave is shown in Fig. 13. According to the comparison of zoomed-in waveforms, the consistency between oscilloscope and NVNA measurements can also be concluded. In order to inspect the significance of baseband measurements, the reconstructed waveform without baseband information is shown in Fig. 14, along with the envelope comparisons. One can clearly see that, the baseband components play an important role of the temporal

waveform reconstruction, which is important to time-domain current and voltage (I-V) analysis.

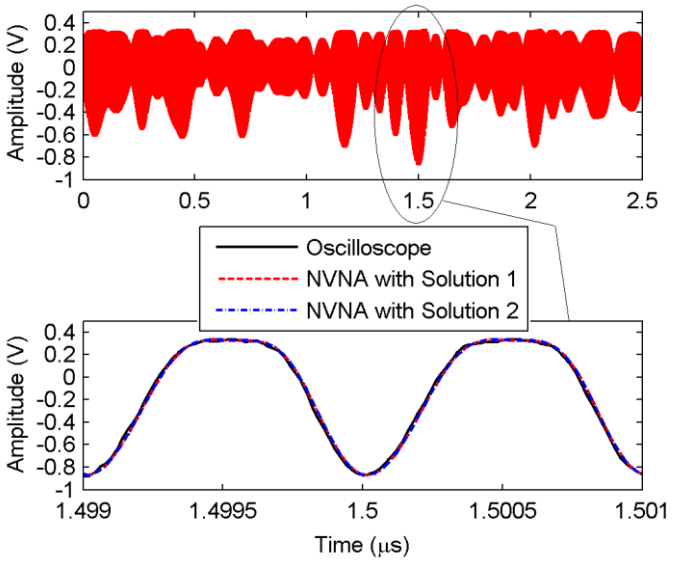

Fig. 13. Comparison between temporal waveform measurements of PA output (B_2) using oscilloscope and NVNA test bench.

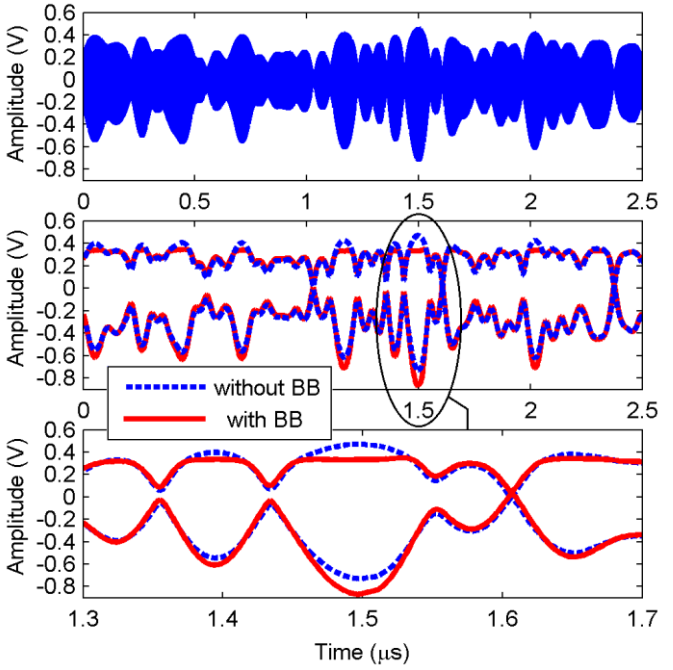

Fig. 14. Waveform reconstruction without baseband information, and envelope comparison.

V. Mixer Characterization

A. NVNA Test Bench Setup

In order to further explore the application of this work, an RF mixer is used as a second type of DUT in this section. Based on the NVNA test bench setup shown in Fig. 15, the intermediate frequency (IF) input and modulated RF output of DUT are, respectively, measured with Port 1 and Port 2. Moreover, a desired phase reference using Solution One in Section III (A) is applied to the Port 3.

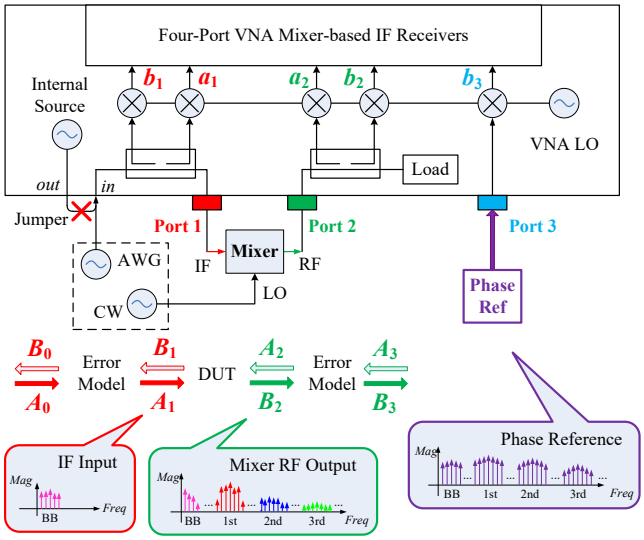

Fig. 15. Illustration of NVNA test bench setup for mixer characterization.

The baseband IF input is generated by the internal arbitrary waveform generator (AWG) of a VSG. To achieve this, the VSG is set to generate the LTE-like multisine in Section IV (A), and outputs baseband in-phase (I) signal to the DUT. Due to the DUT (Mini-Circuit 15542 ZFM-150) specifications, a local oscillator (LO) frequency of 1 GHz is chosen for up-conversion test, which is applied by a continuous wave (CW) generator. As a matter of fact, the AWG and CW generator can be obtained with a single VSG, which works in "Baseband Output *On*, Modulation *Off*, and RF Output *On*" mode.

In this paper, we mainly investigate the mixer behavior when the LO power level sweeps, aiming to present an example of how NVNA test bench can be used for mixer characterization. Without loss of generality, similar NVNA setup can be widely used for mixer down-conversion test, IF/RF level sweep test, and so forth. However, these potential applications are far beyond the main scope of this work, which focuses on the extension of NVNA baseband measurements.

B. Experimental Results

As shown in Fig. 16, the VSG baseband I/Q outputs have a full-scale voltage range of ±1 V. Through the VNA front-panel jumper, the periodical in-phase (I) signal is applied to the DUT IF input port, and kept static during the experiment. To begin the test, the DUT is offered a -15 dBm CW LO, and measured by the NVNA test bench at baseband and harmonic bands. Afterwards, the LO power level increasingly sweeps to 15 dBm on a step of 5 dB. At each LO power level, the input and output of DUT are fully characterized.

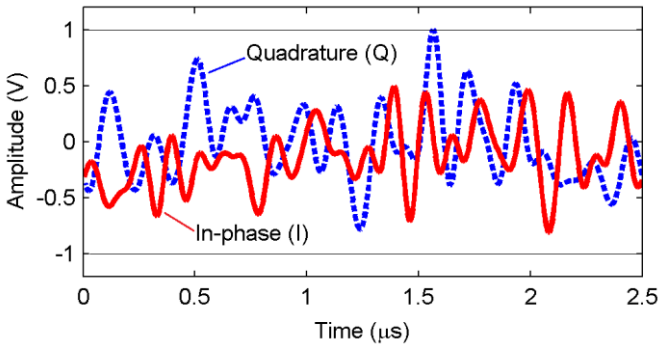

Fig. 16. Waveforms of VSG baseband I/Q outputs, where the in-phase (I) one is applied to the DUT as IF input.

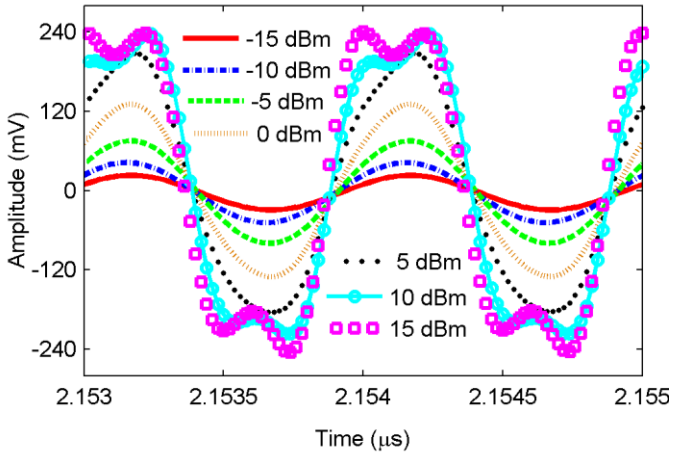

Fig. 18. Zoomed-in waveforms of DUT RF output at all LO power levels.

Parts of the reconstructed waveforms of DUT RF output are given in Fig. 17. One can clearly see that, the baseband components play a significant role when the LO is small, but are negligible when the LO is large. As a matter of fact, the power level of baseband components does not increase with the power sweep of LO (not shown in this paper). According to the results in Fig. 18, however, the DUT starts to show noticeable nonlinear behaviors when the LO is larger than 0 dBm.

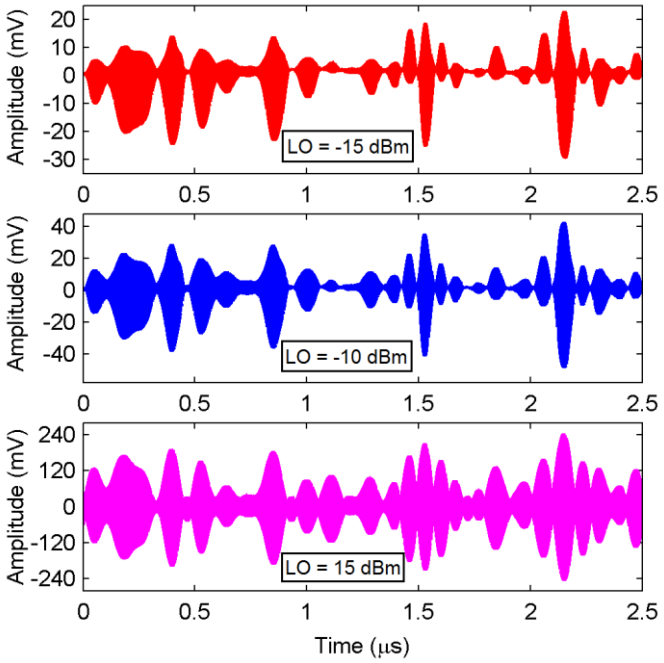

Fig. 17. Reconstructed waveforms of DUT RF output at LO power levels of -15 dBm, -10 dBm, and 15 dBm.

An interesting phenomenon is found in this work when comparing the magnitude and phase results between DUT IF input and RF output. Along with the increase of LO power, the magnitude spectrum of RF components becomes more resemble to that of IF input, as shown in Fig. 19. At the same time, the phase deviation becomes much smaller when the LO is larger than 5 dBm, as shown in Fig. 20. In other words, the DUT shows surprisingly more ideal up-conversion, i.e., moving the very IF components (with specific magnitude and phase relationships) to the target RF band, when it works on nonlinear mode. From another point, the harmonic nonlinearity of carriers brings in no "distortion" but "correction" to the up-conversion, for the very DUT and under the very experimental condition of this work.

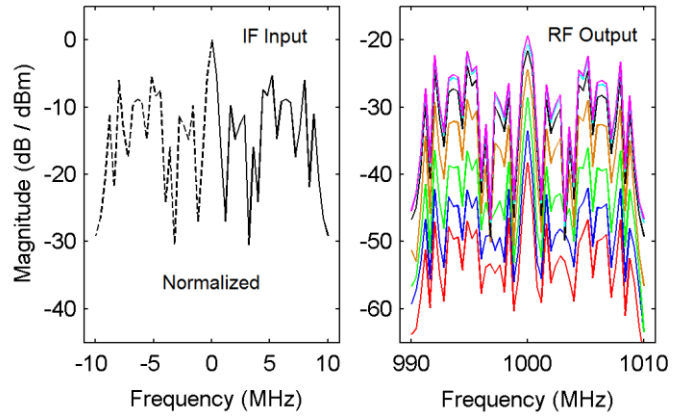

Fig. 19. Comparison between magnitude spectra of mixer IF input (A_1) and RF output (B_2) at different LO levels.

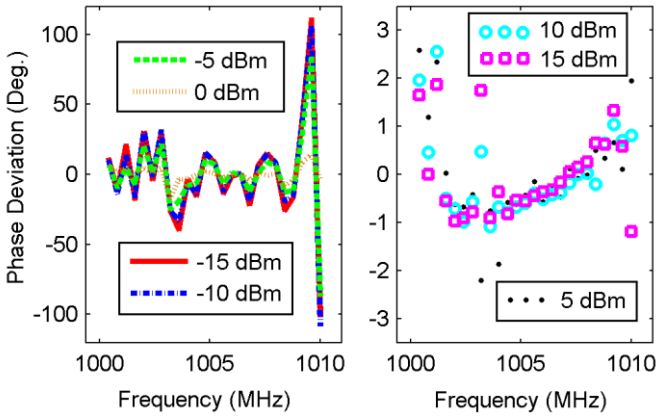

Fig. 20. Phase deviation between mixer IF input (A_1) and RF output (B_2) at different LO levels.

From our point of view, the DUT time-domain behavior causing dominant baseband contribution (as shown in Fig. 17) might be a potential explanation of this phenomenon. Besides, the distinct odd/even harmonic behaviors (not shown in this paper) of DUT might also be relevant. Due to the main scope of this paper, however, the weird nonlinear behavior of DUT is not further analyzed or modeled here. From the perspective of application, the proposed NVNA test bench can be found useful for mixer characterization and modeling under complex modulation, since full-band spectral components of the DUT input and output can be measured for various frequency- and time-domain analysis.

VI. Discussion

A. Uncertainty and Error Analysis

In order to evaluate the phase measurement uncertainty of proposed NVNA test bench, four kinds of dominant contribution should be taken into consideration, including

(i) uncertainty of dual-band phase standard values,
(ii) uncertainty of measurements during phase calibration,
(iii) uncertainty of raw DUT measurements,
(iv) and uncertainty of phase alignment.

In our previous work [16] [17], the uncertainty analysis for the four kinds of contribution has been fully discussed in details. On the basis of that, the analysis of (ii) and (iii) in this paper will deepen the discussion of phase reference stability.

For the first solution of phase reference in Section III (A), the short-term phase instability arising from random noise is about than ±0.2 deg. inside each test band. Due to the drift of carrier phases, however, a long-term bidirectional phase offset exists between the baseband and multi-harmonic components, which is about ±0.3 deg./min at 1 GHz. Given our experience, the time cost of a complete PA or mixer test (including phase calibration) is generally less than 5 min under program control. As a result, the long-term phase instability from calibration to DUT test can be estimated as ±1.5 deg. at maximum in the unidirectional drift case. In Table I, the worst-case uncertainty arising from phase reference stability is evaluated.

TABLE I
Uncertainty Budget of Phase Reference Stability (Solution One)

Uncertainty Sources	Standard Uncertainty (Deg.)
Short-term random noise	0.2
Long-term phase drift	0.9

For the second solution in Section III (B), the short-term phase instability arising from multisine noise is also ±0.2 deg. inside each test band. When using a single comb generator to provide the auxiliary reference on coarse grids, the long-term phase drift discussed above can be neglected from our point of view, since the harmonic phases are equivalently static. In this case, the random noise of auxiliary reference will result in another uncertainty contribution of ±0.2 deg. through the phase alignment processing in (5) and (6). While if the auxiliary reference is obtained by combining two signals together, the similar long-term phase drift will be involved as well, along with the contribution through phase alignment. As a result, the uncertainty arising from phase reference stability in this case can be evaluated as in Table II.

TABLE I
Uncertainty Budget of Phase Reference Stability (Solution Two)

Uncertainty Sources	Standard Uncertainty (Deg.)
Short-term multisine ref noise	0.2
Short-term auxiliary ref noise	0.2
Long-term phase drift (conditional)	0.9

Despite all this, a phase accuracy of ±2 deg. has been experimentally derived for the dominant measurements in this paper. According to the results in Fig. 12, an accuracy level of ±5 deg. should be easily achievable in practice from our perspectives. As a matter of fact, such frequency-domain measurement accuracy does not influence much, if any, for the time-domain waveform reconstruction and analysis given our experience.

B. Phase Reference

As mentioned in Section III (A), the performance (e.g., the bandwidth, spectral grid, and power level) of proposed phase reference approaches can be widely adjusted by selecting satisfactory modulated signals. In addition to the detailed discussions made in [16] and [17], which apply to both phase reference approaches proposed, here we would like to discuss about the selection of reference signals from the application perspectives.

For the first approach in Section III (A), pulsed-RF signals are more convenient for narrowband conditions in our opinion, since one does not need to design the complex multisine and control the VSGs. When a limited number of VSGs are available, the pulsed-RF signals can still be easily obtained with analog signal generators. As a result, only one VSG is needed for the NVNA test bench, providing the complex modulated test stimuli. While for wideband conditions on dense spectral grids,

where hundreds or even thousands of tones are under test, multisine signals could be chosen to improve the achievable tone number and spectral level.

Compared with the first solution, the second approach in Section III (B) is more suitable for wideband conditions where a limited number of VSGs are available. In this case, the desired tone number and spectral level can be simply achieved using the primary phase reference of sweeping multisine. When it comes to the auxiliary phase reference, several methods are optional in practice, for examples:

(i) using a commercial NVNA comb generator on a 10-MHz spectral grid [21];

(ii) using a CW-driven SRD comb generator on a 100-MHz (adjustable to a certain extent) spectral grid [22];

(iii) combining the 10-MHz reference of test bench with a CW-driven SRD comb generator on 1-GHz (adjustable to a certain extent) spectral grid [22];

(iv) and combining the multiple VNA internal sources working on CW mode with desired frequencies.

C. VNA Unit

In order to achieve the NVNA test bench with desired baseband measurement, the VNA unit should meet the following requirements at the same time:

(i) low-frequency measurement range down to tens or at least hundreds of kHz, so that the baseband components can be measured;

(ii) configurable source and receiver channel access, so that the external modulated stimuli can be applied;

(iii) and multiple measurement ports (up to five or more synchronous receivers) available, so that a two-port DUT and the phase reference can be measured at the same time.

To the best of our knowledge, however, only a few commercial VNA models are satisfactory in these aspects. As a result, the achievable densest spectral grid and highest RF bandwidth in practice are limited accordingly at this time.

VII. CONCLUSION

The extension of NVNA baseband measurement is inspected in this paper. To achieve that, two kinds of phase reference approaches are proposed as alternative solutions. Based on these techniques, the NVNA test bench can be used for PA characterization under full baseband, multi-harmonic, and inter-modulation distortion, so that the complete behavior of DUT can be measured and investigated. As another potential type of DUT for the NVNA test benches, an RF mixer under complex modulation is also tested for example to explore the application of this work, whose performance of up-conversion is analyzed based on full-band measurements. In conclusion, the proposed NVNA techniques can be widely used for the full characterization of RF PAs and mixers in practice, which is supportive for the analysis and modeling researches.

REFERENCES

[1] P. Blockley, D. Gunyan, and J. Scott, "Mixer-Based, Vector-Corrected, Vector Signal/Network Analyzer Offering 300kHz-20GHz Bandwidth and Traceable Phase Response," in *2005 IEEE MTT-S International Microwave Symposium Digest*, pp.1497-1500, Jun 2005.

[2] T. Gasseling, E. Gartard, C. Charbonniaud, and A. Xiong, "Assets of source pull for NVNA based load pull measurements," in *79th ARFTG Microwave Measurement Conference Digest*, pp. 1-5, Jun. 2012.

[3] A.M. Pelaez-Perez, S. Woodington, M. Fernandez-Barciela, P. Tasker, and J. Alonso, "Application of an NVNA-Based System and Load-Independent X-Parameters in Analytical Circuit Design Assisted by an Experimental Search Algorithm," *IEEE Transactions on Microwave Theory and Techniques*, vol. 61, no. 1, pp. 581-586, Jan. 2013.

[4] H. Jang, A. Zai, T. Reveyrand, P. Roblin, Z. Popovic, and D. E. Root, "Simulation and measurement-based X-parameter models for power amplifiers with envelope tracking," in *2013 IEEE MTT-S International Microwave Symposium Digest*, pp.1-4, Jun. 2013.

[5] L. Gomme and Y. Rolain, "A reference signal for a dense frequency grid phase calibration," in *Proceedings of the IEEE Instrumentation and Measurement Technology Conference*, pp. 49-53, May 2008.

[6] M. Mirra, M. Marchetti, F. Tessitor, M. Spirito, L. C. N. de Vreede, and L. Betts, "A multi-step phase calibration procedure for closely spaced multi-tone signals," in *75th ARFTG Microwave Measurement Conference Digest*, pp. 1-5, May 2010.

[7] J. Hu, K.G. Gard, and M.B. Steer, "Calibrated non-linear vector network measurement without using a multi-harmonic generator," *IET Microwave, Antennas & Propagation*, vol. 5, no. 5, pp. 616-624, 2011.

[8] Y. Rolain, M. Schoukens, R. Pintelon, and G. Vandersteen, "Synchronizing modulated NVNA measurements on a dense spectral grid," in *79th ARFTG Microwave Measurement Conference Digest*, pp. 1-3, Jun. 2012.

[9] Y. Zhang and M. Lin, "A New NVNA Phase Reference for Poly-harmonic Inter-modulation Measurements," *IEEE Transactions on Instrumentation and Measurement*, vol. 62, no. 6, pp. 1467-1672, Jun. 2013.

[10] F. Verbeyst, M.V. Bossche, and G. Paillonc, "Next generation comb generators for accurate modulated measurements," in *81st ARFTG Microwave Measurement Conference Digest*, pp. 1-4, Jun. 2013.

[11] S. Ahmed, F. Verbeyst, and M.V. Bossche, "A Phase Calibration Methodology for Accurate Modulated Measurements," in *82nd ARFTG Microwave Measurement Conference Digest*, pp. 1-6, Nov. 2013.

[12] Y. Zhang, Z. He, H. Li, and M. Nie, "Dense spectral grid NVNA phase measurements using Vector Signal Generators," *IEEE Transactions on Instrumentation and Measurement*, vol. 63, no. 12, pp. 2983-2992, Dec. 2014.

[13] D. Ribeiro, P. Cruz, and N. Crvalho, "Towards a denser frequency grid in phase measurements using mixer-based receivers," in *85th ARFTG Microwave Measurement Conference Digest*, pp. 1-5, May 2015.

[14] J. Verspecht, "Generation and Measurement of a Millimeter-Wave Phase Dispersion Reference Signal based on a Comb Generator," in *2016 IEEE MTT-S International Microwave Symposium Digest*, pp.1-4, Aug. 2016.

[15] M. Rejeb, A. Raslan, and S. Boumaiza, "Phase Calibration for Coherent Multi-Harmonic Modulated Signal Measurements Using Nonlinear Vector Network Analyzer," in *2016 IEEE MTT-S International Microwave Symposium Digest*, pp.1-4, Aug. 2016.

[16] Y. Zhang, X. Guo, Z. He, H. Huang, J. Huang, M. Nie, L. Wang, A. Yang, and Z. Lu, "Characterization for Multi-harmonic Inter-modulation Nonlinearity of RF Power Amplifiers using a Calibrated Nonlinear Vector Network Analyzer," *IEEE Transactions on Microwave Theory and Techniques*, vol. 64, no. 9, pp.2912–2923, Sep. 2016.

[17] Y. Zhang, X. Guo, Z. He, L. Wang, A. Yang, M. Nie, and M. Liu, "Characterizing Dual-band RF PAs Using Wideband Synchronization and Calibration Techniques of Nonlinear Vector Network Analyzer," *IEEE Transactions on Microwave Theory and Techniques*, vol. 64, no. 11, pp.3934–3945, Nov. 2016.

[18] P. Blockley, J. Scott, D. Gunyan, and A. Parker, "The Random Component of Mixer-Based Nonlinear Vector Network Analyzer Measurement Uncertainty," *IEEE Transactions on Microwave Theory and Techniques*, vol. 55, no. 10, pp. 2231-2239, Oct. 2007.

[19] W.V. Moer, and Y.Rolain, "A Large-Signal Network Analyzer: Why Is It Needed," *IEEE Microwave Magazine*, pp. 46-61, Dec. 2006

[20] M. Lin, and Y. Zhang, "Covariance-matrix-based uncertainty analysis for NVNA measurements," *IEEE Transactions on Instrumentation and Measurement*, vol. 61, no. 1, pp. 93-102, Jan. 2012.

[21] Keysight Technologies, U9391C/F/G Comb Generators, Technical Overview 5989-7619EN, August 2014. Available: http://literature.cdn.keysight.com/litweb/pdf/5989-7619EN.pdf
[22] Herotek, Step Recovery Diode Comb (Harmonic) Generators. Available: http://www.herotek.com/datasheets/pdf/Step_Recovery_Diode_Comb_(Harmonic)_Generators_01-26GHz.pdf

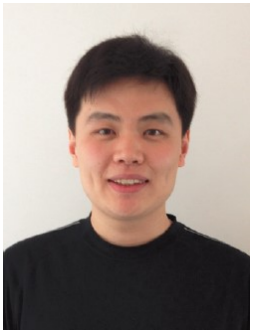

Yichi Zhang (M' 14) received the Ph.D. degree in the Harbin Institute of Technology, Harbin, China, in 2013. He is currently with the RF Parameter Laboratory, Division of Electronics and Information Technology, National Institute of Metrology, Beijing, China. His research interests include the RF phase measurement, complex modulated signal characterization, calibration techniques and uncertainty analysis of the NVNA, and the measurement-based nonlinear behavioral modeling.

Xiaotao Guo (M' 14) received his Ph.D. degree in 2013 from Beijing University of Posts and Telecommunications. He is currently with the RF Parameter Laboratory, Division of Electronics and Information Technology, National Institute of Metrology, Beijing, China. His main research interests include electromagnetic reverberation chamber, and simulation of complex wireless channels.